RESEARCH ARTICLE

The role of cranial osteoderms on the mechanics of the skull in scincid lizards

Arsalan Marghoub[1] | **Loïc Kéver[2]** | **Catherine J. A. Williams[3,4]** |
Arkhat Abzhanov[5] | **Matthew Vickaryous[4]** | **Anthony Herrel[2]** |
Susan E. Evans[6] | **Mehran Moazen[1]**

[1]Department of Mechanical Engineering, University College London, London, UK

[2]Département Adaptations du Vivant, Bâtiment, UMR 7179 MECADEV C.N.R.S/M.N.H.N, d'Anatomie Comparée, Paris, France

[3]Department of Biology, Aarhus University, Aarhus C, Denmark

[4]Department of Biomedical Sciences, University of Guelph, Guelph, Ontario, Canada

[5]Department of Life Sciences, Faculty of Natural Sciences, Imperial College London, Silkwood Park Campus, Berkshire, UK

[6]Centre for Integrative Anatomy, Department of Cell and Developmental Biology, University College London, London, UK

Correspondence
Mehran Moazen, Department of Mechanical Engineering, University College London, London WC1E 7JE, UK.
Email: m.moazen@ucl.ac.uk

Funding information
Human Frontier Science Program, Grant/Award Number: RGP0039/2019

Abstract

Osteoderms (ODs) are calcified organs formed directly within the skin of most major extant tetrapod lineages. Lizards possibly show the greatest diversity in ODs morphology and distribution. ODs are commonly hypothesized to function as a defensive armor. Here we tested the hypothesis that cranial osteoderms also contribute to the mechanics of the skull during biting. A series of in vivo experiments were carried out on three specimens of *Tiliqua gigas*. Animals were induced to bite a force plate while a single cranial OD was strain gauged. A finite element (FE) model of a related species, *Tiliqua scincoides*, was developed and used to estimate the level of strain across the same OD as instrumented in the in vivo experiments. FE results were compared to the in vivo data and the FE model was modified to test two hypothetical scenarios in which all ODs were (i) removed from, and (ii) fused to, the skull. In vivo data demonstrated that the ODs were carrying load during biting. The hypothetical FE models showed that when cranial ODs were fused to the skull, the overall strain across the skull arising from biting was reduced. Removing the ODs showed an opposite effect. In summary, our findings suggest that cranial ODs contribute to the mechanics of the skull, even when they are loosely attached.

KEYWORDS
biomechanics, craniofacial system, feeding, mechanical strain, *Tiliqua*

1 | INTRODUCTION

Osteoderms (ODs) are calcified organs formed directly within the skin of major extant tetrapod lineages including amphibians (various frog species), mammals (such as the armadillo), and reptiles (turtles, crocodilians, and many lizards—e.g., Vickaryous & Sire, 2009). Lizards,

with over 7,000 species, show the greatest diversity in OD morphology and distribution (e.g., Williams et al., 2022). When present, ODs vary in shape, size, and body-wide distribution (e.g., Broeckhoven et al., 2015, 2016; Kever et al., 2022; Kirby et al., 2020; Maisano et al., 2019; Moss, 1969). Among lizards, ODs may be present across the entire body; be restricted to one region of the body,

like the head; or be entirely absent. Morphologically, ODs may resemble a series of overlapping plates, non-overlapping elements forming articulating mosaics, or polymorphic spicules that thicken with age (Laver et al., 2020; Vickaryous & Sire, 2009; Williams et al., 2022).

ODs are most commonly hypothesized to function as a defensive armor, whether against predators, aggressive prey, or conspecifics (e.g., Broeckhoven, 2022; Chen et al., 2015; Liang et al., 2021; Yang et al., 2013). Several alternative hypotheses related to their role and function have been proposed, including thermoregulation (e.g., due to their vascularization), reinforcement of the axial skeleton, or mineral storage and availability (e.g., Broeckhoven, De Kock, & Mouton, 2017; Broeckhoven, du Plessis, & Hui, 2017; Lissethe et al., 2022; Losos et al., 2002; Seidel, 1979). An additional hypothesis considering ODs within the cranial system is that they may contribute to the biomechanics of the skull, reducing the level of strain across the skull during biting or enabling the animals to bite harder (Xue et al., 2017).

Finite element (FE) method is a powerful tool that has been widely used to investigate the biomechanics of the craniofacial system in the field of functional morphology (e.g., Dutel et al., 2021; Moazen et al., 2009a,b; Nieto et al., 2021; O'Higgins et al., 2012; Rayfield, 2007; Richmond et al., 2005). Several studies have highlighted the importance of validation of these models (e.g., Gröning et al., 2013; Kupczik et al., 2007) where validated models can be used to test a number of hypothetical scenarios. This approach can allow us to investigate the role and function of ODs in the cranial system and to test the hypothesis that ODs contribute to the mechanics of the skull.

Scincidae is one of the largest and most widely distributed groups of lizards (e.g., Abbate et al., 2009; Koppetsch et al., 2021; Shea, 2004). Lizards of the genus *Tiliqua* are large-bodied members of this family with several species having relatively broad-heads and blue-tongues. They are widespread in Australia, Indonesia and New Guinea and are omnivorous with enlarged and blunt posterior teeth possibly used for crushing hard foods (e.g., Abbate et al., 2009; Wilson, 2012). *Tiliqua gigas* and *Tiliqua scincoides* are two closely related species with almost identical craniofacial morphologies. In addition, both have a similar mosaic-like arrangement of compound ODs covering their skulls (see e.g., Kever et al., 2022). The mechanics of their feeding has been investigated by several authors and it is well established that they use their tongue and jaw to capture their prey (e.g., Abbate et al., 2009; Herrel et al., 1998a, 1998b; Hewes & Schwenk, 2021). They seem ideal species to test

the role and function of ODs on the mechanics of the skull.

Our overall aim was to study the role of cranial osteoderms on the mechanics of the skull in *T. gigas* and *T. scincoides*. To test the hypothesis that ODs that are closely connected to the cranial bones reduce the level of mechanical strain across the skull arising from biting, we first carried out a series of in vivo studies measuring bite force and mechanical strain on a temporal OD of three *T. gigas*. We then developed a generic finite element model of a *Tiliqua* based on a specimen of *T. scincoides* and estimated the level of strain across an OD homologous with that of *T. gigas* to the one investigated during the in vivo experiments. Finally, we used the FE models to test two hypothetical scenarios under which all ODs and their associated soft tissues were (i) removed from or (ii) fused to, the skull. In both scenarios the level of mechanical strain across the skull was characterized.

2 | MATERIALS AND METHODS

A series of experimental in vivo measurements were carried out to quantify the level of mechanical strain across a single osteoderm of *T. gigas*. These experimental data were used to validate a finite element model that was developed to model the in vivo experiments. Following the comparison between the finite element model and in vivo results further finite element simulations were carried out to model two hypothetical scenarios that could not be tested experimentally.

2.1 | In vivo testing

2.1.1 | Collection of the in vivo data

Three *T. gigas* (both 47–48 mm in head length) were purchased from the commercial pet shop "La Ferme Tropicale" in Paris (France). For the in vivo experiment, *T. gigas* were used as substitutes for *T. scincoides*, because the former was more readily available. The two species are morphologically similar (only postcranial differences have been reported), and they are considered subspecies of a single species by some authors (see e.g., Koppetsch et al., 2021; Shea, 2004).

All individuals were lightly anesthetized (ketamine 80 mg/kg), the epidermis was removed from the osteoderm after which it was cleaned and degreased using hydrogen peroxide. Next, a rectangular strain gauge rosette (C5K-06-S5198-350-33F, Micro-Measurements, Raleigh, NC) was glued on a large osteoderm located

near the middle of the temporal area of each individual using super glue (Figure 1a). The ODs were instrumented with the gauges following the protocol described in Ross et al. (2018). Once animals fully recovered from the anesthesia, they were manually restrained and induced to bite on a custom-made bite force transducer (see Herrel et al., 1999).

For each individual, the bite plates of the transducer were placed between the jaws of the animal at the front and back of the mouth. The back bites were recorded on the ipsilateral and contralateral side of the instrumented osteoderm. The bite points throughout the text will refer to the aforementioned bite points as frontal, ipsilateral and contralateral. Strain and bite force data were recorded simultaneously and amplified using Vishay (Vishay Precision Group Micro-Measurements, Raleigh, NC) 2310 bridge- and Kistler (Kistler Instrument Corp, Novi, MI) 5011B charge-amplifiers, respectively. The outputs of both amplifiers were routed to an analogue to numeric converter (MP 150, BIOPAC systems, Goleta, CA) and recorded at a sampling rate of 1.0 kHz (BIOPAC systems).

2.1.2 | Analysis of the in vivo data

Force and strain signals were first calibrated and filtered using a lowpass filter with a cut-off frequency between 100 and 150 Hz. Then maximal principal strains (i.e., maximal tensile strain in the plane of the gauge) and minimal principal strains (i.e., maximal compressive strain in the plane of the gauge) were calculated using custom-written procedures (IGOR Pro 6.0 WaveMetrics, Inc., Lake Oswego, OR). Finally, the peak force value and the associated strains were recorded and saved for each bite using another custom-written Igor procedure.
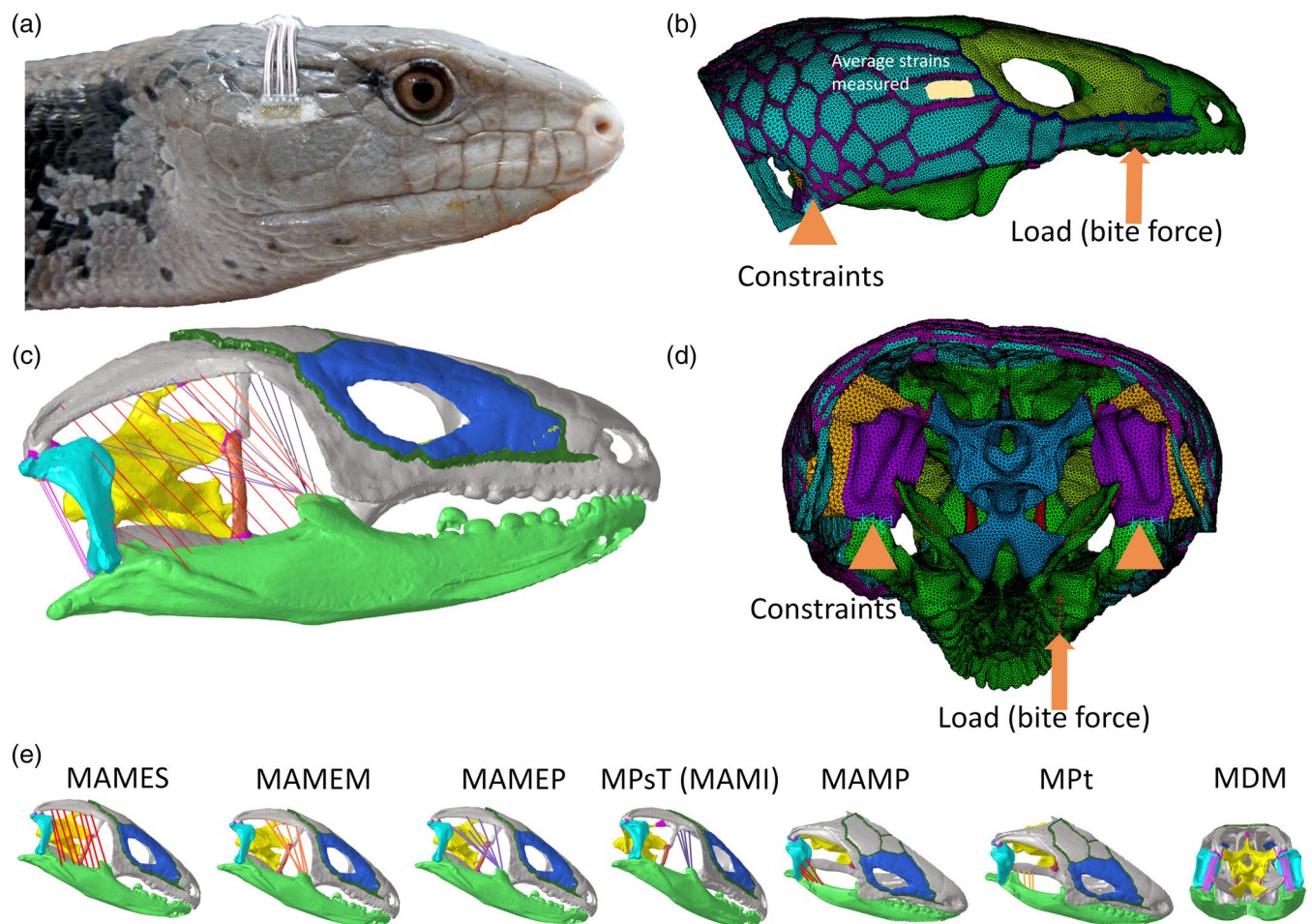

FIGURE 1 Lateral view of the in vivo strain gauged *Tiliqua gigas* highlighting the exact position of the strain gauge (a). Loading and boundary conditions applied while modeling the lateral biting force of *Tiliqua scincoides* (b–e). Note, (c) and (e) show the line of action of the considered muscle groups on the model. These include: *MAMES*: m. adductor mandibulae externus superfcialis (anterior and posterior sections); *MAMEM*: m. adductor mandibulae externus medialis; *MAMEP*: m. adductor mandibulae externus profundus; *MPsT*: m. pseudotemporalis (combining superficialis and profundus); *MAMP*: m. adductor mandibulae posterior; *MPt*: m. pterygoideus (combining lateralis and medialis); *MDM*: m. depressor mandibulae

2.2 | In silico testing

2.2.1 | Model development

Avizo Lite 9.2 (ThermoFisher Scientific) was used to reconstruct the microCT images of a head of *T. scincoides* with the head length of 47.7 mm, downloaded from Morphosource. A 3D model was then developed, which consisted of multiple components including osteoderms (ODs) separated by connective tissue between the skull, the braincase, and the quadrates (Figure 1b). Then, the 3D volumetric mesh of ca. 1,200,000 tetrahedral elements was imported into a commercial finite element package, ANSYS Mechanical APDL 19.0 (Canonsburg). The connective tissues were meshed with ca. 330,000 elements, skull bones were meshed with ca. 640,000 elements and the ODs were meshed with ca. 230,000 elements.

2.2.2 | Loads and boundary conditions

Muscle forces reported by Herrel et al. (1998a, 1998b) were incorporated into the FE model. In short, the line of action of the muscles was determined and maximum muscle forces per muscle group were estimated and applied to the skull (Figure 1c,d, see also Table S1). Carrying out a detailed multibody dynamic analysis (e.g., Curtis et al., 2008; Moazen et al., 2008) to estimate the muscle forces was beyond the scope of this study. Instead, the focus was to estimate the maximum muscle forces and develop a model as close as possible to our in vivo measurements. Next, the in vivo measured bite forces of *T. gigas* were applied to the model. Boundary conditions were applied at the quadratomandibular joints where four nodes were constrained in all degrees of freedom (Figure 1e).

2.2.3 | Material properties and simulations

All connective tissues were modeled with an elastic modulus of 10 MPa (see e.g., Henderson et al., 2005; Moazen et al., 2015) whereas bones and osteoderms were modeled with an elastic modulus of 10 GPa (e.g., Moazen et al., 2013; Moazen et al., 2009a,b). Poisson's ratio of 0.3 was used for all materials. We are conscious of the heterogeneous properties of osteoderms (Marghoub et al., 2022) and bone and the viscoelastic nature of soft tissues, but consider that the aforementioned properties could provide a reasonable estimate of the different material properties, considering the overall aim of this study.

Two sets of simulations were performed: (1) 12 models were developed corresponding to 12 different bites based on the bite forces measured in one animal, that is three bite points each repeated four times during the in vivo experiments. Here, the maximum muscle forces (same values applied in all cases) and specific bite force per bite were applied to the model and the level of strain at the strain gauged OD was compared between the FE model and in vivo data corresponding to the animal studied; (2) the model corresponding to a specific bite point (ipsilateral) based on the aforementioned simulation was used to model two hypothetical scenarios in which all ODs and their associated soft tissues were (i) removed from or (ii) fused to, the skull. The fusion of the ODs to the skull was modeled by adjusting the elastic modulus of the connective tissues from 10 MPa to 10 GPa (i.e., same as bone properties). Here, the levels of strain across the ODs and skull and connective tissues was compared between the aforementioned hypothetical scenarios and the corresponding baseline model.

3 | RESULTS

Experimental in vivo strain gauging showed that the examined ODs were always loaded during maximum bites. Results corresponding to one animal (that was used to compare vs. FE data) are included in Table 1. Results obtained from the other animals are included in the Appendix and those data show a similar pattern. The level of experimentally measured strain varied across different bites. Anterior bites led to a lower level of bite force and strain across the OD whereas the posterior bites led to a higher level of bite force and strain across the OD (Tables 1 and S2).

Comparison of the in vivo measured strain data to the in silico predictions overall revealed a similar pattern across different bite points. Nonetheless, experimental strains were consistently higher than the in silico predictions. For example, considering the baseline model (ipsilateral bite with a bite force of 169.8 N), maximum (P1) and minimum (P3) principal strains measured experimentally were 3,184, and −2,431 microstrain where the FE predictions were 1,699 and −1,385 microstrain respectively, that is, 47 and 43% difference between the experimental and FE results (Table 1). This difference reached a maximum of 204 and 58% for lateral contralateral and frontal bites, respectively.

The hypothetical FE models demonstrated that the level of connection between the ODs and the adjacent bone can considerably impact the pattern of strain distribution across the skull during biting. Fusing all ODs to the skull led to a considerable reduction of the von Mises strain across the skull, compared to the baseline model. Removing the ODs showed an opposite effect, that is, this

TABLE 1 Strain values measured (in microstrain) virtually compared with the experimental values to validate the finite element model

	Bite force (N)	In vivo		In silico		% Δ	
		P1	P3	P1	P3	P1	P3
Ipsilateral	169.9	3,183.7	−2,431.5	1,698.8	−1,384.6	46.6	43.1
	164.4	2000.5	−688.5	1,576.0	−1,277.1	21.2	85.5
	151.5	1760.1	−740.5	1,436.4	−1,139.3	18.4	53.9
	151.5	3,496.4	−2,905.5	1,436.4	−1,139.3	58.9	60.8
Contralateral	144.4	1,172.4	−259.6	863.3	−790.3	26.4	204.4
	140.3	694.1	−315.9	817.6	−742.3	17.8	134.9
	133.3	752.7	−337.5	739.9	−660.5	1.7	95.7
	129.7	891.7	−424.1	699.8	−618.3	21.5	45.8
Frontal	133.5	1,555.5	−876.1	1,433.8	−1,203.5	7.8	37.4
	127.5	1,307.7	−700.1	1,336.3	−1,109.4	2.2	58.5
	124.7	2066.9	−1,359.0	1,290.9	−1,065.5	37.5	21.6
	118.3	2,305.0	−1,438.1	1,187.1	−965.3	48.5	32.9

Note: Experimental measurements were recorded at several bite forces with different biting positions and correspond to only one individual that was used for the purpose of comparison with the finite element model. Note P1 and P3 correspond to maximum and minimum principal strains.
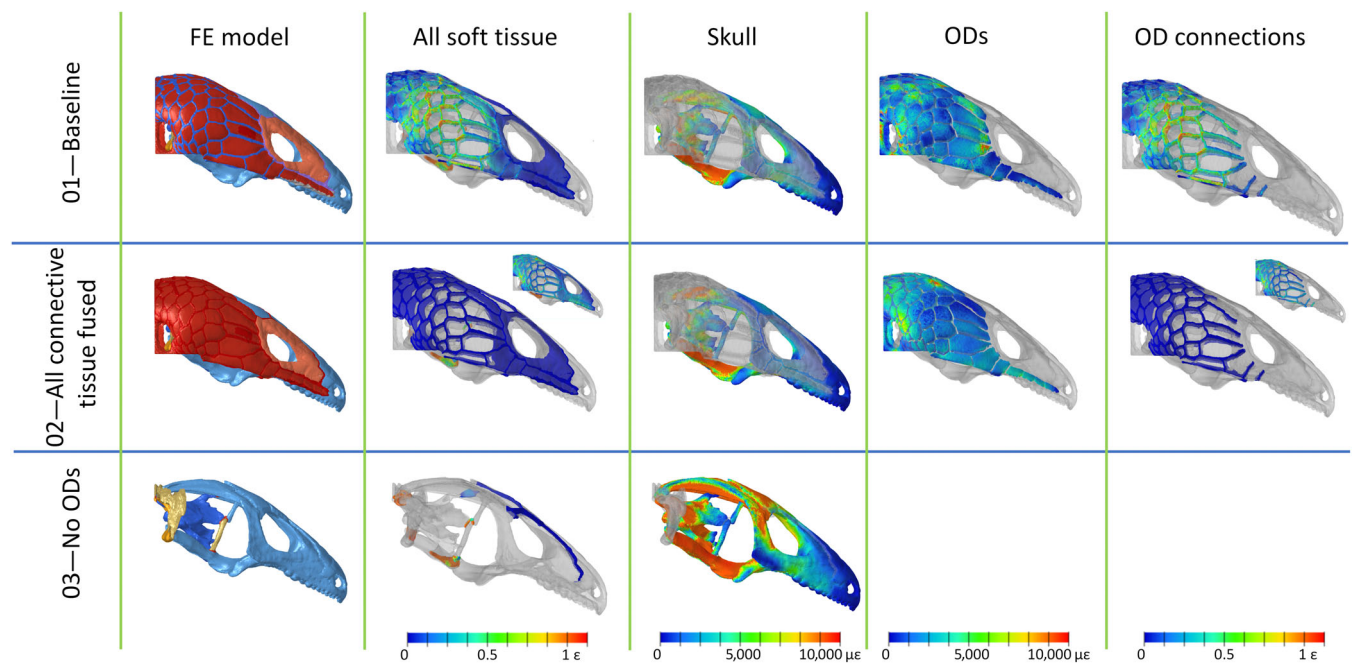

FIGURE 2 Lateral view of the pattern of von Mises strain distribution across different components of the model. We investigated three simulated scenarios: baseline (which is the natural model with connective tissue sutures between the bones—01 baseline), fused connections between osteoderm–osteoderm and osteoderm–skull (02—all connective tissue fused), and all osteoderms virtually removed (03—no ODs). Note the loading on the FE models correspond to the ipsilateral bite

resulted in an increase in the level of von Mises strain across the skull (Figures 2–4). In other words, this demonstrated that ODs in the baseline model (i.e., their natural connection to the skull) reduce the level of strain across the skull. The reduction in the level of strain due to the presence of ODs (i.e., comparing the Baseline vs. the No ODs models in Figures 2–4) were notable, especially across the orbit, jugal, parietal, posterior frontal and pterygoid, whereas there was little impact on the epipterygoid and premaxilla where overall levels of strain were low.

It is worth noting that the baseline model showed a rather uniform distribution of the von Mises strain
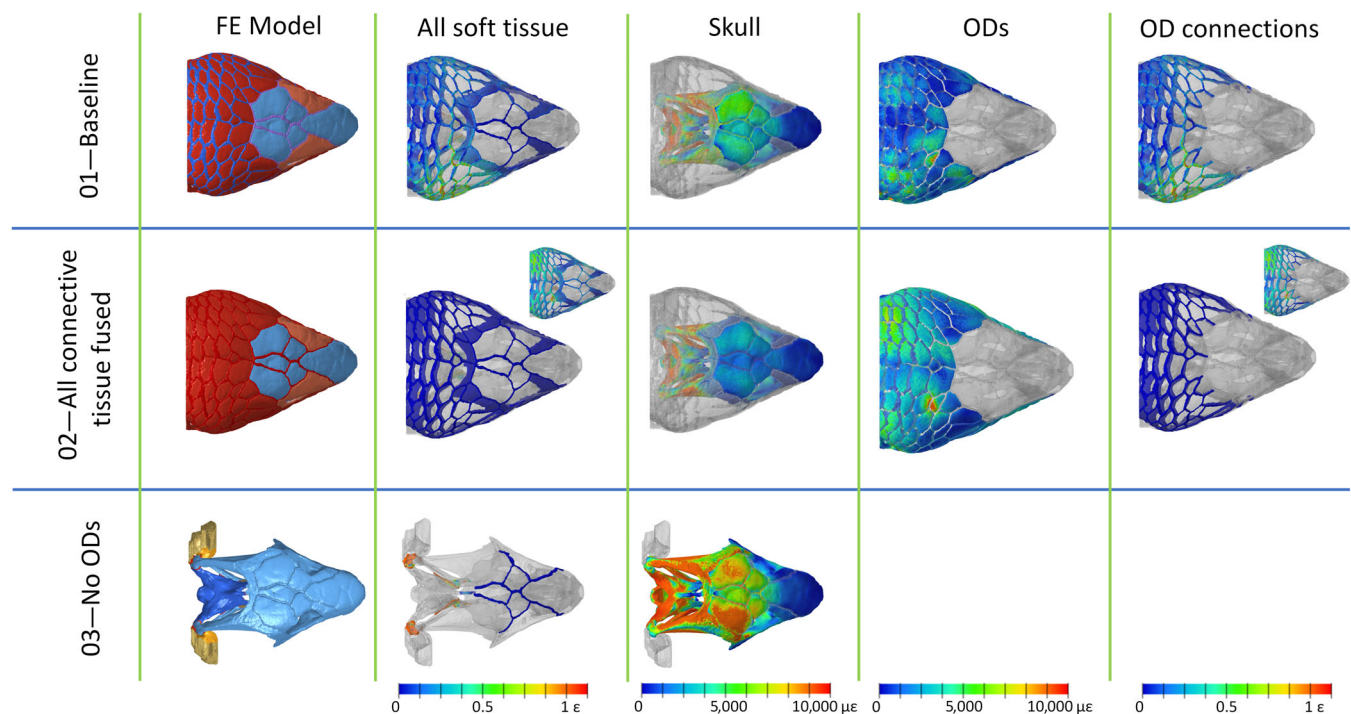
FIGURE 3 Dorsal view of the pattern of von Mises strain distribution across different components of the model. We investigated three simulated scenarios: baseline (which is the natural model with connective tissue sutures between the bones—01 baseline), fused connections between osteoderm–osteoderm and osteoderm–skull (02—all connective tissue fused), and all osteoderms virtually removed (03—no ODs). Note the loading on the FE models correspond to the ipsilateral bite

across all the soft connective tissue connecting the ODs to the skull (in response to biting). When all soft tissues were ossified, fusing the ODs to the skull bones (their elastic modulus increased to that of the bone), they undertook a lower level of loading, increasing the overall stiffness of the skull (i.e., reducing the strain across the skull).

4 | DISCUSSION

Osteoderms are widely considered to act as a protective armor for intra- or interspecies competition while various authors have proposed other functions such as thermoregulation or mineral storage (e.g., Broeckhoven, 2022; Broeckhoven, De Kock, & Mouton, 2017; Broeckhoven, du Plessis, & Hui, 2017; de Buffrénil et al., 1986; Lissethe et al., 2022; Losos et al., 2002; Seidel, 1979). Our results reveal that, in *Tiliqua*, cranial ODs are loaded during biting and, depending on their level of attachment/fusion to the underlying skull, also contribute to the mechanics of the skull (see also Xue et al., 2017). Taken together, our data support the prediction that cranial ODs have roles beyond strictly protective armor (e.g., Broeckhoven, De Kock, & Mouton, 2017; Broeckhoven, du Plessis, & Hui, 2017; Stanley, 2013, 2016).

In a hypothetical scenario where all ODs were fused together and to the underlying skull, our FE models demonstrate that the overall strain across the skull arising from biting would be reduced (see Figures 3 and 4 for the "skull" column). Skeletal fusion will naturally increase the robustness of the skull, potentially enabling the animal to bite harder. This could be a functional adaptation to the local environment/food sources, allowing the lizard to bite harder or defend itself better against a predator. Nonetheless, it comes at a cost that is, reducing the flexibility of the head as a whole. A similar explanation has been proposed for the fusion of cranial sutures (in lizards) where fusion can at least locally reduce the level of strain on the adjacent bones (Moazen et al., 2013; Moazen et al., 2009a,b). The lower temporal bar has been suggested to function similarly, as a complete bar can potentially increase the overall rigidity of the skull (Herrel et al., 2007; Moazen et al., 2009a). On the other hand, the soft tissues connecting the ODs can act as shock absorbers that might be helpful during encounters with conspecifics, predators or aggressive prey (e.g., Broeckhoven et al., 2016; Jaslow & Biewner, 1995). Similarly, when we completely removed the ODs from the *Tiliqua* skull, the level of strain across the skull was increased in comparison to the natural/baseline scenario, reinforcing the argument that cranial
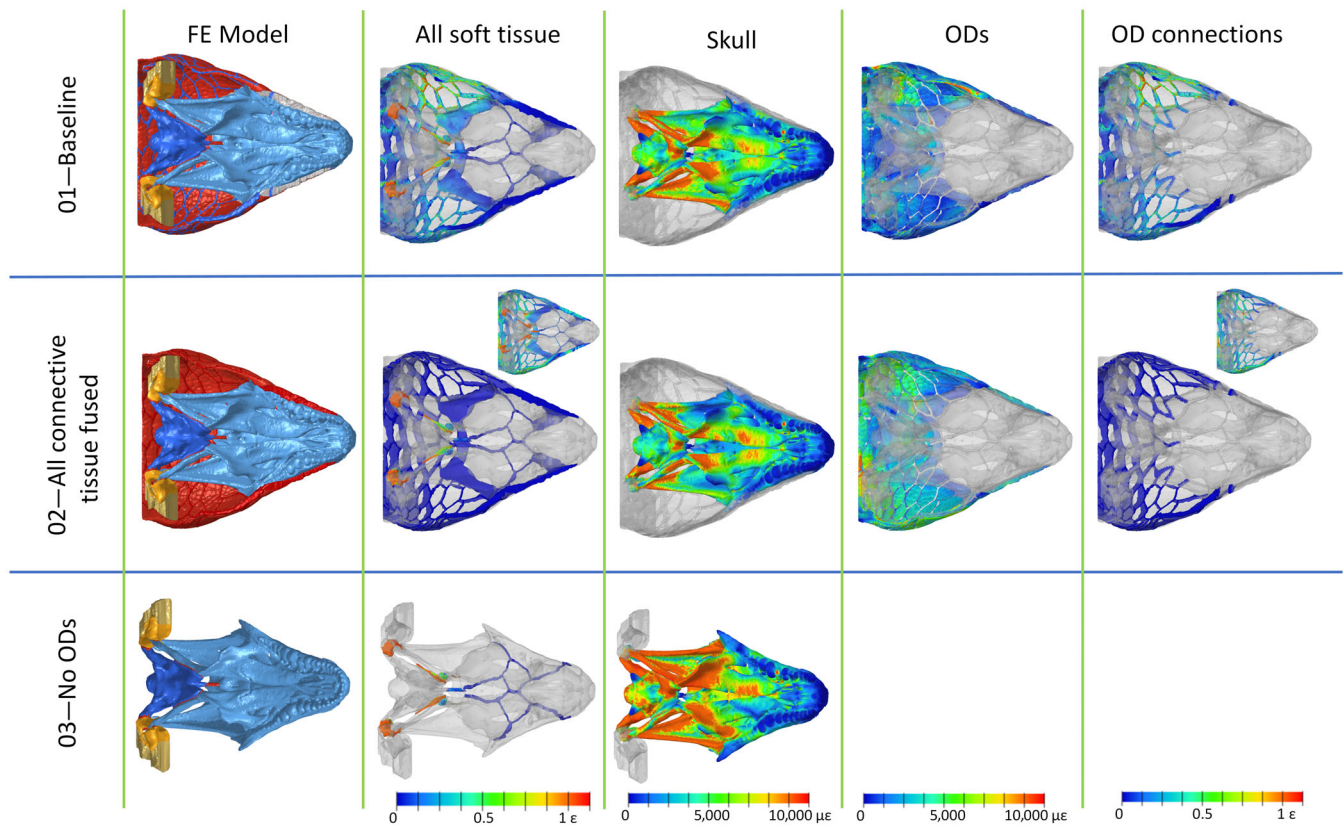
FIGURE 4 Ventral view of the pattern of von Mises strain distribution across different components of the model. We investigated three simulated scenarios: baseline (which is the natural model with connective tissue sutures between the bones—01 baseline), fused connections between osteoderm–osteoderm and osteoderm–skull (02—all connective tissue fused), and all osteoderms virtually removed (03—no ODs). Note the loading on the FE models correspond to the ipsilateral bite

ODs can impact the mechanics of the skull even when they are not fused to one another or to underlying cranial bone. An alternative scenario that was not included in this study is the case of ODs being modeled as soft tissues (instead of being completely removed). This scenario is likely to have led to results in between the two extreme scenarios modeled in this study, with for example, the level of strain across the skull being higher than the scenario in which all ODs were removed and lower that the scenario in which all ODs were fused to the skull.

Several key questions remain to be answered. For example, what drives ODs to become fused or loosely attached to the underlying bones in lizards, to what extent does the nano- and micro-structural variation of the ODs themselves (Iacoviello et al., 2020; Marghoub et al., 2022) impact skull mechanics, whether compound osteoderms (multiple smaller elements or osteodermites forming an OD) so commonly found in other skinks would behave differently than the large and robust non-compound osteoderms (see e.g., Kever et al., 2022; Liang et al., 2021) found in *Tiliqua rugosa*? These adaptations are likely impacted by a combination of natural selection and developmental constraints that will require a much

wider investigation across lizards in an evolutionary framework (e.g., Broeckhoven et al., 2016; Vickaryous et al., 2022).

The finite element model developed in this study had several limitations. First, it was not an individual-specific FE model. Second, the loading applied to the skull did not correspond to the maximum muscle forces in all cases. Third, the compound ODs of *T. gigas* and *T. scincoides* were modeled as single non-compound ODs, not taking into account the micro-motions that might be present at the interface of osteodermites. These limitations can explain the large differences that we observed between the in vivo strain gauge data and the FE predictions. Nonetheless, despite the limitations of the model presented here, we consider that the relative comparison made between the hypothetical and baseline models developed here remain valid.

In summary, our findings suggest that cranial ODs can contribute to the mechanics of the skull. As expected, the attachment of the ODs to the underlying bone can contribute to a reduction in cranial strain as it increases the overall rigidity of the skull. However, significantly, both our experimental and modeling results demonstrate

that the presence of loosely connected ODs also contributes to a reduction in cranial strain. It is clear that loosely connected ODs have a larger flexibility while ODs fused to the skull bones can enhance the overall stiffness of the skull. Further work is required to understand the epi/genetic factors contributing to the level of attachment of ODs to their adjacent bones.

AUTHOR CONTRIBUTIONS

Arsalan Marghoub: Data curation; formal analysis; investigation; methodology; validation; visualization; writing – original draft; writing – review and editing. **Loïc Kéver:** Data curation; formal analysis; investigation; methodology; validation; visualization; writing – original draft; writing – review and editing. **Catherine Williams:** Investigation; writing – review and editing. **Arkhat Abzhanov:** Conceptualization; funding acquisition; project administration; writing – review and editing. **Matthew Vickaryous:** Funding acquisition; methodology; project administration; resources; software; supervision; validation; visualization; writing – review and editing. **Anthony Herrel:** Funding acquisition; methodology; project administration; resources; software; supervision; validation; visualization; writing – review and editing. **Susan Evans:** Funding acquisition; methodology; project administration; resources; software; supervision; validation; visualization; writing – review and editing. **Mehran Moazen:** Funding acquisition; methodology; project administration; resources; software; supervision; validation; visualization; writing – review and editing.

ACKNOWLEDGEMENT

CONFLICT OF INTEREST STATEMENT

The authors declare no potential conflict of interests.

ETHICS STATEMENT

All experimental procedures were approved by the University of Antwerp Ethics Committee (reference 2006/18).

ORCID

Arsalan Marghoub https://orcid.org/0000-0002-0839-576X

Catherine J. A. Williams https://orcid.org/0000-0002-4839-6134

Matthew Vickaryous https://orcid.org/0000-0002-0093-0895

Anthony Herrel https://orcid.org/0000-0003-0991-4434

Susan E. Evans https://orcid.org/0000-0002-0799-4154

Mehran Moazen https://orcid.org/0000-0002-9951-2975

REFERENCES

Abbate, F., Latella, G., Montalbano, G., Guerrera, M. C., Germanà, G. P., & Levanti, M. B. (2009). The lingual dorsal surface of the blue-tongue skink (*Tiliqua scincoides*). *Anatomia, Histologia, Embryologia*, *38*, 348–350.

Broeckhoven, C. (2022). Intraspecific competition: A missing link in dermal armour evolution? *The Journal of Animal Ecology*, *91*(8), 1562–1566.

Broeckhoven, C., De Kock, C., & Mouton, P. L. F. N. (2017). Sexual dimorphism in osteoderm expression and the role of male intrasexual aggression. *Biological Journal of the Linnean Society*, *122*, 329–339.

Broeckhoven, C., Diedericks, G., Hui, C., Makhubo, B. G., & Mouton, P. L. (2016). Enemy at the gates: Rapid defensive trait diversification in an adaptive radiation of lizards. *Evolution; International Journal of Organic Evolution*, *70*(11), 2647–2656.

Broeckhoven, C., Diedericks, G., & Mouton, P. (2015). What doesn't kill you might make you stronger: Functional basis for variation in body armour. *The Journal of Animal Ecology*, *84*(5), 1213–1221.

Broeckhoven, C., du Plessis, A., & Hui, C. (2017). Functional trade-off between strength and thermal capacity of dermal armor: Insights from girdled lizards. *Journal of the Mechanical Behavior of Biomedical Materials*, *74*, 189–194.

Chen, I. H., Yang, W., & Meyers, M. A. (2015). Leatherback sea turtle shell: A tough and flexible biological design. *Acta Biomaterialia*, *28*, 2–12.

Curtis, N., Kupczik, K., O'Higgins, P., Moazen, M., & Fagan, M. J. (2008). Predicting skull loading: Applying multibody dynamics analysis to a macaque skull. *The Anatomical Record*, *291*, 491–501.

de Buffrénil, V., Farlow, J. O., & de Ricqlés, A. (1986). Growth and function of *Stegosaurus* plates: Evidence from bone histology. *Paleobiology*, *12*, 459–473.

Dutel, H., Gröning, F., Sharp, A. C., Watson, P. J., Herrel, A., Ross, C. F., Jones, M. E. H., Evans, S. E., & Fagan, M. J. (2021). Comparative cranial biomechanics in two lizard species: Impact of variation in cranial design. *The Journal of Experimental Biology*, *224*, jeb234831.

Gröning, F., Jones, M. E., Curtis, N., Herrel, A., O'Higgins, P., Evans, S. E., & Fagan, M. J. (2013). The importance of accurate muscle modelling for biomechanical analyses: A case study with a lizard skull. *Journal of the Royal Society, Interface*, *10*, 20130216.

Henderson, J. H., Chang, L. Y., Song, H. M., Longaker, M. T., & Carter, D. R. (2005). Age-dependent properties and quasi-static strain in the rat sagittal suture. *Journal of Biomechanics*, *38*, 2294–2301.

Herrel, A., Aerts, P., & De Vree, F. (1998a). Static biting in lizards: Functional morphology of the temporal ligaments. *Journal of Zoology*, *244*, 135–143.

Herrel, A., Aerts, P., & De Vree, F. (1998b). Ecomorphology of the lizard feeding apparatus: A modelling approach. *Netherlands Journal of Zoology*, *48*, 1–25.

Herrel, A., De Vree, F., Delheusy, V., & Gans, C. (1999). Cranial kinesis in gekkonid lizards. *The Journal of Experimental Biology*, *202*, 3687–3698.

Herrel, A., Schaerlaeken, V., Meyers, J. J., Metzger, K. A., & Ross, C. F. (2007). The evolution of cranial design and performance in squamates: Consequences of skull-bone reduction on

feeding behavior. *Integrative and Comparative Biology*, *47*, 107–117.

Hewes, A. E., & Schwenk, K. (2021). The functional morphology of lingual prey capture in a scincid lizard, *Tiliqua scincoides* (Reptilia: Squamata). *Journal of Morphology*, *282*, 127–145.

Iacoviello, F., Kirby, A. C., Javanmardi, Y., Moeendarbary, E., Shabanli, M., Tsolaki, E., Sharp, A. C., Hayes, M. J., Keevend, K., Li, J. H., Brett, D. J., Shearing, P. R., Olivo, A., Herrmann, I. K., Evans, S. E., Moazen, M., & Bertazzo, S. (2020). The multiscale hierarchical structure of *Heloderma suspectum* osteoderms and their mechanical properties. *Acta Biomaterialia*, *107*, 194–203.

Jaslow, C. R., & Biewner, A. A. (1995). Strain patterns in the horn-cores, cranial bones and sutures of goats (*Capra hircus*) during impact loading. *Journal of Zoology London*, *235*, 193–210.

Kever, L., Olivier, D., Marghoub, A., Evans, S. E., Vickaryous, M. K., Moazen, M., & Herrel, A. (2022). Biomechanical behaviour of lizard osteoderms and skin under external loading. *The Journal of Experimental Biology*, *225*, jeb244551.

Kirby, A., Vickaryous, M., Boyde, A., Olivo, A., Moazen, M., Bertazzo, S., & Evans, S. (2020). A comparative histological study of the osteoderms in the lizards *Heloderma suspectum* (Squamata: Helodermatidae) and *Varanus komodoensis* (Squamata: Varanidae). *Journal of Anatomy*, *236*, 1035–1043.

Koppetsch, T., Wantania, L. L., Boneka, F. B., & Böhme, W. (2021). Crossing the weber line: First record of the giant blue-tongue skink *Tiliqua gigas* (Schneider, 1801) (Squamata: Scincidae) from Sulawesi, Indonesia. *Bonn Zoological Bulletin*, *69*, 185–189.

Kupczik, K., Dobson, C. A., Fagan, M. J., Crompton, R. H., Oxnard, C. E., & O'Higgins, P. (2007). Assessing mechanical function of the zygomatic region in macaques: Validation and sensitivity testing of finite element models. *Journal of Anatomy*, *210*, 41–53.

Laver, R. J., Morales, C. H., Heinicke, M. P., Gamble, T., Longoria, K., Bauer, A. M., & Daza, J. D. (2020). The development of cephalic armor in the Tokay gecko (Squamata: Gekkonidae: *Gekko gecko*). *Journal of Morphology*, *281*, 213–228.

Liang, C., Marghoub, A., Kever, L., Bertazzo, S., Abzhanov, A., Vickaryous, M., Herrel, A., Evans, S., & Moazen, M. (2021). Lizard osteoderms—Morphological characterisation, biomimetic design and manufacturing based on three species. *Bioinspiration & Biomimetics*, *16*, 066011.

Lissethe, L., Veenstra, I., & Broeckhoven, C. (2022). Revisiting the thermoregulation hypothesis of osteoderms: A study of the crocodilian *Paleosuchus palpebrosus* (Crocodilia: Alligatoridae). *Biological Journal of the Linnean Society*, *135*, 679–691.

Losos, J. B., Mouton, P. L. F. N., Bickel, R., Cornelius, I., & Ruddock, L. (2002). The effect of body armature on escape behaviour in cordylid lizards. *Animal Behaviour*, *64*, 313–321.

Maisano, J. A., Laduc, T. J., Bell, C. J., & Barber, D. (2019). The cephalic osteoderms of *Varanus komodoensis* as revealed by high-resolution x-ray computed tomography. *The Anatomical Record*, *302*, 1675–1680.

Marghoub, A., Williams, C. J. A., Vasco Leite, J., Kirby, A. C., Kever, L., Porro, L. B., Barrett, P. M., Bertazzo, S., Abzhanov, A., Vickaryous, M., Herrel, A., Evans, S. E., & Moazen, M. (2022). Unravelling the structural variation of lizard osteoderms. *Acta Biomaterialia*, *46*, 306–316.

Moazen, M., Costantini, D., & Bruner, E. (2013). A sensitivity analysis to the role of fronto-parietal suture in *Lacerta bilineata*: A preliminary finite element approach. *The Anatomical Record*, *296*, 198–209.

Moazen, M., Curtis, N., Evans, S. E., O'Higgins, P., & Fagan, M. J. (2008). Rigid-body analysis of a lizard skull: Modelling the skull of *Uromastyx hardwickii*. *Journal of Biomechanics*, *41*, 1274–1280.

Moazen, M., Curtis, N., O'Higgins, P., Evans, S. E., & Fagan, M. J. (2009a). Biomechanical assessment of evolutionary changes in the lepidosaurian skull. *Proceedings of the National Academy of Sciences of the United States of America*, *106*, 8273–8277.

Moazen, M., Curtis, N., O'Higgins, P., Jones, M. E. H., Evans, S. E., & Fagan, M. J. (2009b). Assessment of the role of sutures in a lizard skull—A computer modelling study. *Proceedings of the Royal Society, Part B*, *276*, 39–46.

Moazen, M., Peskett, E., Babbs, C., Pauws, E., & Fagan, M. J. (2015). Mechanical properties of calvarial bones in a mouse model for craniosynostosis. *PLoS One*, *12*(10), e0125757. https://doi.org/10.1096/fasebj.2022.36.S1.R3199

Moss, M. L. (1969). Comparative histology of dermal sclerifications in reptiles. *Acta Anatomica*, *73*, 510–533.

Nieto, M. N., Degrange, F. J., Sellers, K. C., Pol, D., & Holliday, C. M. (2021). Biomechanical performance of the cranio-mandibular complex of the small notosuchian *Araripesuchus gomesii* (Notosuchia, Uruguaysuchidae). *Anatomical Record*, *305*(10), 2695–2707.

O'Higgins, P., Fitton, L. C., Phillips, R., Shi, J. F., Liu, J., Gröning, F., Cobb, S. N., & Fagan, M. J. (2012). Virtual functional morphology: Novel approaches to the study of craniofacial form and function. *Evolutionary Biology*, *39*, 521–535.

Rayfield, E. J. (2007). Finite element analysis and understanding the biomechanics and evolution of living and fossil organisms. *Annual Review of Earth and Planetary Sciences*, *35*, 541–576.

Richmond, B. G., Wright, B. W., Grosse, I., Dechow, P. C., Ross, C. F., Spencer, M. A., & Strait, D. S. (2005). Finite element analysis in functional morphology. *The Anatomical Record*, *283*, 259–274.

Ross, C. F., Porro, L. B., Herrel, A., Evans, S. E., & Fagan, M. J. (2018). Bite force and cranial bone strain in four species of lizards. *The Journal of Experimental Biology*, *221*, jeb180240.

Seidel, M. R. (1979). The osteoderms of the American alligator and their functional significance. *Herpetologica*, *35*, 375–380.

Shea, G. M. (2004). History and systematics. In R. Hitz, M. S. Glenn, A. Hauschild, K. Henle, & H. Werning (Eds.), *Blue-tongued skinks: Contributions to Tiliqua and Cyclodomorphus* (pp. 11–23). Matthias Schmidt Publications.

Stanley, E. L. (2013). *Systematics and morphological diversification of the Cordylidae (Squamata)* [Unpublished thesis]. The Richard Gilder Graduate School.

Stanley, E. L. (2016). A review of *Cordylus machadoi* (Squamata: Cordylidae) in southwestern Angola, with the description of a new species from the Pro-Namib desert. *Zootaxa*, *4061*, 201–226.

Vickaryous, M., Williams, C., Willan, G., Kirby, A., Herrel, A., Kever, L., Moazen, M., Marghoub, A., Rai, S., Abzhanov, A., & Evans, S. (2022). Histological diversity and evolution of lizard osteoderms. *The FASEB Journal*, *36*. https://doi.org/10.1096/fasebj.2022.36.S1.R3199

Vickaryous, M. K., & Sire, J. Y. (2009). The integumentary skeleton of tetrapods: Origin, evolution, and development. *Journal of Anatomy*, *214*, 441–464.

Williams, C., Kirby, A., Marghoub, A., Kever, L., Ostashevskaya-Gohstand, S., Bertazzo, S., Moazen, M., Abzhanov, A., Herrel, A., Evans, S. E., & Vickaryous, M. (2022). A review of the osteoderms of lizards (Reptilia: Squamata). *Biological Reviews*, *97*, 1–19.

Wilson, S. (2012). *Australian lizards: A natural history*. CSIRO Publishing.

Xue, J., Marghoub, A., Bertazzo, S., Evans, S. E., & Moazen, M. (2017). Biomechanics of osteoderms in a lizard skull—A preliminary finite element study. *Journal of Anatomy*, *B18*. https://doi.org/10.1111/joa.12637

Yang, W., Chen, I. H., Gludovatz, B., Zimmermann, E. A., Ritchie, R. O., & Meyers, M. A. (2013). Natural flexible dermal armor. *Advanced Materials*, *25*, 31–48.

SUPPORTING INFORMATION

Additional supporting information can be found online in the Supporting Information section at the end of this article.